Indoor Path Planning for Multiple Unmanned Aerial Vehicles via Curriculum Learning

Jongmin Park
School of Integrated Technology
Yonsei University
Incheon, Korea
jm97@yonsei.ac.kr

Kwansik Park*
Korea Aerospace Research Institute
Daejeon, Korea
kspark6469@kari.re.kr
* Corresponding author

Abstract—**Multi-agent reinforcement learning was performed in this study for indoor path planning of two unmanned aerial vehicles (UAVs). Each UAV performed the task of moving as fast as possible from a randomly paired initial position to a goal position in an environment with obstacles. To minimize training time and prevent the damage of UAVs, learning was performed by simulation. Considering the non-stationary characteristics of the multi-agent environment wherein the optimal behavior varies based on the actions of other agents, the action of the other UAV was also included in the state space of each UAV. Curriculum learning was performed in two stages to increase learning efficiency. A goal rate of 89.0% was obtained compared with other learning strategies that obtained goal rates of 73.6% and 79.9%.**

Index Terms—**indoor path planning, multi-agent reinforcement learning, curriculum learning, unmanned aerial vehicle (UAV)**

I. INTRODUCTION

The usage of unmanned aerial vehicles (UAVs) is widespread [1]–[4]. Among them, the quadcopter [5]–[8] is one of the most commonly used UAVs, and it has the advantage of being able to hover and rotate as required. There are various methods for estimating the location of a UAV, such as techniques utilizing global navigation satellite systems (GNSS) [9]–[17], long-term evolution (LTE) signals [18]–[27], enhanced long-range navigation (eLoran) system [28]–[36], and various other techniques [37]–[41]. Additionally, depth cameras, RGB cameras, lidar, and radar can be installed on UAVs for collision avoidance. UAVs can be used in search missions, aerial photography, delivery, airspace management, and communications relays [42]–[45].

Owing to the wide use-cases of UAVs, controlling them autonomously using artificial intelligence (AI) techniques has been studied extensively [46]–[49]. Among them, reinforcement learning is used to learn the optimal behavior in each situation through a reward. It is mainly used in the fields of robotics and game AI and has been widely used owing to recent developments in deep learning.

In this study, we used reinforcement learning on two quadcopters to find the fastest route to a target location while avoiding obstacles. To reduce learning time and cost, and eliminate the risk of damage to the real quadcopter, learning was conducted through simulation in a virtual environment. The indoor virtual environment was implemented using Gazebo [50], which is an open-source 3D robotics simulator. Additionally, to improve learning performance, curriculum learning [51] was conducted in two stages.

A curriculum learning method teaches an easier task first before teaching a more difficult and complex activity. This approach has benefit in terms of generalization and convergence time. In the first stage of our study, a simple path to fly to a target location in the shortest time in an obstacle-free environment was learned. Thereafter, in the second stage, a relatively complex task of flying to the target location in an obstacle-added environment was learned. Curriculum learning enables more efficient learning compared to learning complex tasks from the beginning.

When other agents are considered as part of the multi-agent environment, there are non-stationary characteristics of the multi-agent environment wherein the optimal behavior varies based on the action of other agents [52]. Thus, we added the action of the other agent to the state space, which is a common practice to consider the non-stationary characteristics [53].

II. VIRTUAL SIMULATION

Our simulation of multiple UAVs in an indoor virtual environment was implemented using Robot Operating System (ROS) [54], Gazebo [50], OpenAI Gym [55], and RLlib. ROS is an open source meta-operating system for robotics applications [54]. It was used in this study because it is widely used in the robotics field and can be easily combined with various robot software frameworks. By using the topic communication, which is a message-passing method within ROS, sensor and location information obtained by each UAV were introduced into the learning environment of itself or of the other UAV.

To implement an indoor virtual environment, a single-floor structure of 30 m × 30 m was created using Gazebo's internal tool, the building editor. Figs. 1(a) and 1(b) show the obstacle-free environment used in the first curriculum learning stage and the obstacle-added environment used in the second curriculum learning stage, respectively. Figs. 1(c) and 1(d) illustrate the start and goal position candidates for the UAVs, which are indicated by red squares.

OpenAI Gym is an open-source Python library that contains reinforcement learning algorithms [55]. In OpenAI Gym, vari-
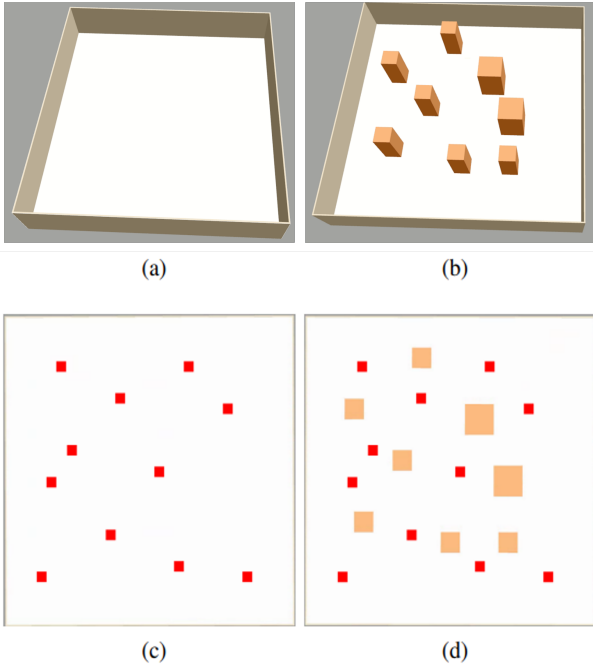
Fig. 1. Indoor virtual environment

ous standard learning environments are provided as references. A new learning environment was implemented in this study according to the learning environment format of OpenAI Gym. OpenAI Gym can be easily linked with PyTorch, TensorFlow, or RLlib [56] which is a reinforcement learning algorithm library.

III. LEARNING ENVIRONMENT

The learning time was divided into *step*, *episode*, and *iteration*. A step is defined as the time to choose an action and obtain a reward and it is the minimum time unit. An episode refers to the time required for the task to succeed or fail, and an iteration updates the model parameters when the episodes have sufficiently progressed.

The size of one iteration is determined by the *train batch size* parameter, which was selected as 20,000 steps in this study. The first stage of the curriculum learning was progressed for 150 iterations, and thereafter the second stage was continuously learned for 310 iterations.

Proximal policy optimization (PPO) [57], which is a reinforcement learning algorithm based on the policy-gradient method, was used in this study because it is more suitable than reinforcement learning algorithms based on Q-learning such as deep Q-networks [58] for situations with a continuous state space [52], [59]. The RLlib provides the PPO algorithm under the name of PPOTrainer. We used the RLlib and hyperparameter settings of [60].

A. State space

The state space was divided into two parts and the heading, distance, and lidar data were used to determine the environment. The heading to the other UAV, distance to the other UAV,

relative heading of the other UAV, and current action of the other UAV were used to determine its situation. In this study, *heading* means the counterclockwise rotation angle required for the UAV to look at the goal position (in radians). *Distance* means the distance that the UAV needs to move when it is looking at the goal position (in meters).

Considering the non-stationary characteristics in a multi-agent environment, the information and actions of the other UAV were provided, and to determine the differences in learning performance, two models with different state spaces were trained and compared. One included only heading, distance, and lidar data of each UAV in the state space of the corresponding UAV, and the other included additional information and actions of the other UAV in the state space of each UAV.

B. Action space

The action space consisted of forward speeds and yaw rates. The basic forward speed and yaw rates were set to 0.5 m/s, and $\frac{\pi}{12}$ rad/s, respectively. The three forward speeds were 0, 1, and 2 times the default forward speed, and the five yaw rates were -2, -1, 0, 1, and 2 times the default yaw rate. A negative yaw rate means counterclockwise rotation, and a positive yaw rate means clockwise rotation. Because this study assumed a 2D situation, the vertical velocity was set to 0.

C. Reward model

Among the two reward models used in a previous study [60], the one that showed good learning performance was applied to the current study. At the end of each episode, a large positive reward is given if the task succeeds; a large negative reward is given if the task fails. To implement movement towards the goal position as quickly as possible, a negative reward is given to each step. In addition, there are rewards regarding the distance and heading to the goal position. The detailed reward model is given in [60].

IV. SIMULATION RESULTS

In this study, three learning models were trained. Model 1 did not proceed with curriculum learning but learned directly in the obstacle-added environment. Model 2 performed curriculum learning but did not include information and actions of the other agent in the state space. Model 3 included information and actions of the other agent in the state space, and performed curriculum learning.

Fig. 2 shows the goal rate of each iteration for Model 1 as a moving average value. Model 1 was trained for 460 iterations in an environment with obstacles. The goal rates of the previous ten iterations were used to calculate a moving average value. A maximum goal rate of 73.6% was attained by Model 1.

Figs. 3 and 4 show the goal rate of each iteration for Models 2 and 3, respectively, as a moving average value. Models 2 and 3 were trained for 150 iterations in the first curriculum learning stage and additionally trained for 310 iterations in the second stage. Maximum goal rates of 79.9% and 87.0% were
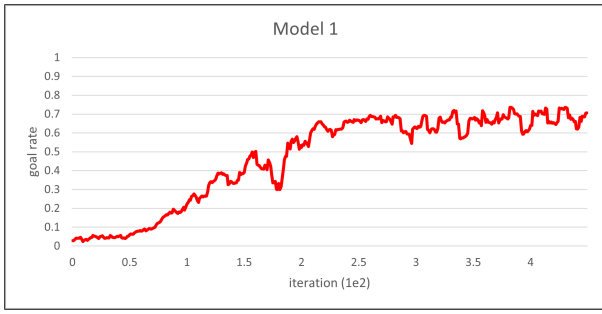
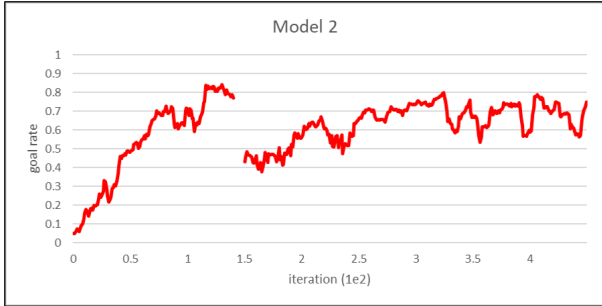Fig. 2. Goal rate for Model 1 as a moving average value

Fig. 3. Goal rate for Model 2 as a moving average value

attained by Models 2 and 3, respectively, in an environment with obstacles.

Model 1, which did not use curriculum learning, directly learned in the obstacle-added environment, and achieved the lowest goal rate. In contrast, Models 2 and 3, which used curriculum learning, achieved relatively high goal rates. Model 2 showed unstable learning progress, which is indicated by the fluctuations of the goal rates in Fig. 3, because of the non-stationary characteristics in a multi-agent environment. Whereas, Model 3, which added information and actions of the other UAV to the state space to consider the non-stationary characteristics, showed stable learning progress compared with Model 2. The maximum goal rates achieved by Models 1, 2, and 3 were 73.6%, 79.9%, and 87.0%, respectively. Therefore, Model 3 performed significantly better than the other two.
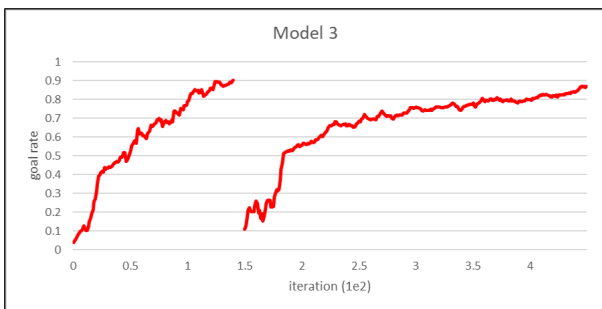

Fig. 4. Goal rate for Model 3 as a moving average value

V. Conclusion

In this study, we performed reinforcement learning for multi-UAV indoor path planning. Curriculum learning was performed in two stages to increase learning efficiency. We showed that the cases with the curriculum learning demonstrated higher goal rates than the other case after the same number of iterations. It was also shown that it is important to include the other agent's information in the state space when a multi-agent environment is considered. When the other agent's information was included in the state space, more stable learning progress and higher goal rates were achievable.

Acknowledgment

References

[1] T. Alladi, Naren, G. Bansal, V. Chamola, and M. Guizani, "SecAuthUAV: A novel authentication scheme for UAV-ground station and UAV-UAV communication," *IEEE Trans. Veh. Technol.*, vol. 69, no. 12, pp. 15 068–15 077, 2020.

[2] H. Lee, T. Kang, and J. Seo, "Development of confidence bound visualization tool for LTE-based UAV surveillance in urban areas," in *Proc. ICCAS*, 2019, pp. 1187–1191.

[3] S. K. Singh, K. Agrawal, K. Singh, C.-P. Li, and W.-J. Huang, "On UAV selection and position-based throughput maximization in multi-UAV relaying networks," *IEEE Access*, vol. 8, pp. 144 039–144 050, 2020.

[4] H. Lee, W. Kim, and J. Seo, "Simulation of UWB radar-based positioning performance for a UAV in an urban area," in *Proc. IEEE ICCE-Asia*, 2018.

[5] N. Xuan-Mung, S. K. Hong, N. P. Nguyen, L. N. N. T. Ha, and T.-L. Le, "Autonomous quadcopter precision landing onto a heaving platform: New method and experiment," *IEEE Access*, vol. 8, pp. 167 192–167 202, 2020.

[6] Y. Shin, S. Lee, and J. Seo, "Autonomous safe landing-area determination for rotorcraft UAVs using multiple IR-UWB radars," *Aerosp. Sci. Technol.*, vol. 69, pp. 617–624, Oct. 2017.

[7] A. Talaeizadeh, H. N. Pishkenari, and A. Alasty, "Quadcopter fast pure descent maneuver avoiding vortex ring state using yaw-rate control scheme," *IEEE Robot. Autom.*, vol. 6, no. 2, pp. 927–934, 2021.

[8] J. Kim, J.-W. Kwon, and J. Seo, "Multi-UAV-based stereo vision system without GPS for ground obstacle mapping to assist path planning of UGV," *Electron. Lett.*, vol. 50, no. 20, pp. 1431–1432, Sep. 2014.

[9] F. Causa and G. Fasano, "Improving navigation in GNSS-challenging environments: Multi-UAS cooperation and generalized dilution of precision," *IEEE Trans. Aerosp. Electron. Syst.*, vol. 57, no. 3, pp. 1462–1479, 2021.

[10] A. K. Sun, H. Chang, S. Pullen, H. Kil, J. Seo, Y. J. Morton, and J. Lee, "Markov chain-based stochastic modeling of deep signal fading: Availability assessment of dual-frequency GNSS-based aviation under ionospheric scintillation," *Space Weather*, vol. 19, no. 9, pp. 1–19, Sep. 2021.

[11] K. Park and J. Seo, "Single-antenna-based GPS antijamming method exploiting polarization diversity," *IEEE Trans. Aerosp. Electron. Syst.*, vol. 57, no. 2, pp. 919–934, Apr. 2021.

[12] C. Savas, G. Falco, and F. Dovis, "A comparative performance analysis of GPS L1 C/A, L5 acquisition and tracking stages under polar and equatorial scintillations," *IEEE Trans. Aerosp. Electron. Syst.*, vol. 57, no. 1, pp. 227–244, 2021.

[13] K. Park, D. Lee, and J. Seo, "Dual-polarized GPS antenna array algorithm to adaptively mitigate a large number of interference signals," *Aerosp. Sci. Technol.*, vol. 78, pp. 387–396, Jul. 2018.

[14] H. Lee, S. Pullen, J. Lee, B. Park, M. Yoon, and J. Seo, "Optimal parameter inflation to enhance the availability of single-frequency GBAS for intelligent air transportation," *IEEE Trans. Intell. Transp. Syst.*, 2022, early access.

[15] H. Lee, J. Seo, and Z. Kassas, "Urban road safety prediction: A satellite navigation perspective," *IEEE Intell. Transp. Syst. Mag.*, 2022, early access.

[16] S. Kim, K. Park, and J. Seo, "Mitigation of GPS chirp jammer using a transversal FIR filter and LMS algorithm," in *Proc. ITC-CSCC*, 2019.

[17] N. Ahmed and J. Seo, "Statistical evaluation of the multi-frequency GPS ionospheric scintillation observation data," in *Proc. ICCAS*, 2017, pp. 1792–1797.

[18] K. Shamaei and Z. M. Kassas, "A joint TOA and DOA acquisition and tracking approach for positioning with LTE signals," *IEEE Trans. Signal Process.*, vol. 69, pp. 2689–2705, 2021.

[19] M. Maaref and Z. M. Kassas, "Ground vehicle navigation in GNSS-challenged environments using signals of opportunity and a closed-loop map-matching approach," *IEEE Trans. Intell. Transp. Syst.*, vol. 21, no. 7, pp. 2723–2738, 2020.

[20] T. Kang, H. Lee, and J. Seo, "Analysis of the maximum correlation peak value and RSRQ in LTE signals according to frequency bands and sampling frequencies," in *Proc. ICCAS*, 2019, pp. 1182–1186.

[21] S. Jeong, H. Lee, T. Kang, and J. Seo, "RSS-based LTE base station localization using single receiver in environment with unknown path-loss exponent," in *Proc. ICTC*, 2020, pp. 958–961.

[22] H. Lee and J. Seo, "A preliminary study of machine-learning-based ranging with LTE channel impulse response in multipath environment," in *Proc. IEEE ICCE-Asia*, 2020.

[23] H. Lee, A. Abdallah, J. Park, J. Seo, and Z. Kassas, "Neural network-based ranging with LTE channel impulse response for localization in indoor environments," in *Proc. ICCAS*, 2020, pp. 939–944.

[24] H. Lee, J. Seo, and Z. Kassas, "Integrity-based path planning strategy for urban autonomous vehicular navigation using GPS and cellular signals," in *Proc. ION GNSS+*, 2020, pp. 2347–2357.

[25] M. Jia, H. Lee, J. Khalife, Z. M. Kassas, and J. Seo, "Ground vehicle navigation integrity monitoring for multi-constellation GNSS fused with cellular signals of opportunity," in *Proc. IEEE ITSC*, 2021, pp. 3978–3983.

[26] T. Kang and J. Seo, "Practical simplified indoor multiwall path-loss model," in *Proc. ICCAS*, 2020, pp. 774–777.

[27] H. Lee, T. Kang, S. Jeong, and J. Seo, "Evaluation of RF fingerprinting-aided RSS-based target localization for emergency response," in *Proc. IEEE VTC*, June 2022.

[28] W. Kim, P.-W. Son, S. G. Park, S. H. Park, and J. Seo, "First demonstration of the Korean eLoran accuracy in a narrow waterway using improved ASF maps," *IEEE Trans. Aerosp. Electron. Syst.*, vol. 58, no. 2, pp. 1492–1496, Apr. 2022.

[29] P.-W. Son, J. Rhee, J. Hwang, and J. Seo, "Universal kriging for Loran ASF map generation," *IEEE Trans. Aerosp. Electron. Syst.*, vol. 55, no. 4, pp. 1828–1842, Oct. 2019.

[30] P.-W. Son, J. Rhee, and J. Seo, "Novel multichain-based Loran positioning algorithm for resilient navigation," *IEEE Trans. Aerosp. Electron. Syst.*, vol. 54, no. 2, pp. 666–679, Oct. 2018.

[31] P. Williams and C. Hargreaves, "UK eLoran–Initial operational capability at the Port of Dover," in *Proc. ION ITM*, 2013, p. 392–402.

[32] W. Kim, P.-W. Son, J. Rhee, and J. Seo, "Development of record and management software for GPS/Loran measurements," in *Proc. ICCAS*, 2020, pp. 796–799.

[33] D. Qiu, D. Boneh, S. Lo, and P. Enge, "Reliable location-based services from radio navigation systems," *Sensors*, vol. 10, no. 12, pp. 11 369–11 389, 2010.

[34] J. Park, P.-W. Son, W. Kim, J. Rhee, and J. Seo, "Effect of outlier removal from temporal ASF corrections on multichain Loran positioning accuracy," in *Proc. ICCAS*, 2020, pp. 824–826.

[35] Y. Li, Y. Hua, B. Yan, and W. Guo, "Research on the eLoran differential timing method," *Sensors*, vol. 20, p. 6518, 2020.

[36] J. H. Rhee, S. Kim, P.-W. Son, and J. Seo, "Enhanced accuracy simulator for a future Korean nationwide eLoran system," *IEEE Access*, vol. 9, pp. 115 042–115 052, Aug. 2021.

[37] E. Kim and J. Seo, "SFOL pulse: A high accuracy DME pulse for alternative aircraft position and navigation," *Sensors*, vol. 17, no. 10, Sep. 2017.

[38] S. Lee, E. Kim, and J. Seo, "SFOL DME pulse shaping through digital predistortion for high-accuracy DME," *IEEE Trans. Aerosp. Electron. Syst.*, vol. 58, no. 3, pp. 2616–2620, June 2022.

[39] J. Rhee and J. Seo, "Low-cost curb detection and localization system using multiple ultrasonic sensors," *Sensors*, vol. 19, no. 6, Mar. 2019.

[40] K. Park, W. Kim, and J. Seo, "Effects of initial attitude estimation errors on loosely coupled smartphone GPS/IMU integration system," in *Proc. ICCAS*, 2020, pp. 800–803.

[41] T. Kang and Y. Shin, "Indoor navigation algorithm based on a smartphone inertial measurement unit and map matching," in *Proc. ICTC*, 2021, pp. 1421–1424.

[42] S. V. Sibanyoni, D. T. Ramotsoela, B. J. Silva, and G. P. Hancke, "A 2-D acoustic source localization system for drones in search and rescue missions," *IEEE Sensors J.*, vol. 19, no. 1, pp. 332–341, 2019.

[43] K. Dorling, J. Heinrichs, G. G. Messier, and S. Magierowski, "Vehicle routing problems for drone delivery," *IEEE Trans. Syst. Man Cybern. Syst.*, vol. 47, no. 1, pp. 70–85, 2017.

[44] T. Hiraguri, K. Nishimori, I. Shitara, T. Mitsui, T. Shindo, T. Kimura, T. Matsuda, and H. Yoshino, "A cooperative transmission scheme in drone-based networks," *IEEE Trans. Veh. Technol.*, vol. 69, no. 3, pp. 2905–2914, 2020.

[45] F. Ho, R. Geraldes, A. Gonçalves, M. Cavazza, and H. Prendinger, "Improved conflict detection and resolution for service UAVs in shared airspace," *IEEE Trans. Veh. Technol.*, vol. 68, no. 2, pp. 1231–1242, 2019.

[46] S. Kouroshnezhad, A. Peiravi, M. S. Haghighi, and A. Jolfaei, "Energy-efficient drone trajectory planning for the localization of 6G-enabled IoT devices," *IEEE Internet Things J.*, vol. 8, no. 7, pp. 5202–5210, 2021.

[47] P. Chhikara, R. Tekchandani, N. Kumar, V. Chamola, and M. Guizani, "DCNN-GA: A deep neural net architecture for navigation of UAV in indoor environment," *IEEE Internet Things J.*, vol. 8, no. 6, pp. 4448–4460, 2021.

[48] S. Kim, J. Park, J.-K. Yun, and J. Seo, "Motion planning by reinforcement learning for an unmanned aerial vehicle in virtual open space with static obstacles," in *Proc. ICCAS*, 2020, pp. 784–787.

[49] J. Lai, K. Cai, Z. Liu, and Y. Yang, "A multi-agent reinforcement learning approach for conflict resolution in dense traffic scenarios," in *IEEE/AIAA DASC*, 2021, pp. 1–9.

[50] N. Koenig and A. Howard, "Design and use paradigms for Gazebo, an open-source multi-robot simulator," in *Proc. IEEE/RSJ IROS*, vol. 3, 2004, pp. 2149–2154.

[51] Y. Bengio, J. Louradour, R. Collobert, and J. Weston, "Curriculum learning," in *Proc. ICPS*, 2009, p. 41–48.

[52] S. Y. Jang, H. J. Yoon, N. S. Park, J. K. Yun, and Y. S. Son, "Research trends on deep reinforcement learning," *Electronics and Telecommunications Trends*, vol. 34, no. 4, pp. 1–14, Aug. 2019.

[53] G. Papoudakis, F. Christianos, A. Rahman, and S. V. Albrecht, "Dealing with non-stationarity in multi-agent deep reinforcement learning," 2019, arXiv:1906.04737.

[54] M. Quigley, K. Conley, B. Gerkey, J. Faust, T. Foote, J. Leibs, R. Wheeler, and A. Ng, "ROS: An open-source robot operating system," in *Proc. ICRA Workshop on Open Source Software*, vol. 3, Jan. 2009.

[55] G. Brockman, V. Cheung, L. Pettersson, J. Schneider, J. Schulman, J. Tang, and W. Zaremba, "OpenAI Gym," Jun. 2016, arXiv:1606.01540.

[56] E. Liang, R. Liaw, R. Nishihara, P. Moritz, R. Fox, K. Goldberg, J. Gonzalez, M. Jordan, and I. Stoica, "RLlib: Abstractions for distributed reinforcement learning," in *Proc. ICML*, vol. 80, Jul. 2018, pp. 3053–3062.

[57] J. Schulman, F. Wolski, P. Dhariwal, A. Radford, and O. Klimov, "Proximal policy optimization algorithms," Jul. 2017, arXiv:1707.06347.

[58] V. Mnih, K. Kavukcuoglu, D. Silver, A. Graves, I. Antonoglou, D. Wierstra, and M. Riedmiller, "Playing Atari with deep reinforcement learning," 2013, arXiv:1312.5602.

[59] M. Klissarov, P.-L. Bacon, J. Harb, and D. Precup, "Learnings options end-to-end for continuous action tasks," Nov. 2017, arXiv:1712.00004.

[60] J. Park, S. Jang, and Y. Shin, "Indoor path planning for an unmanned aerial vehicle via curriculum learning," in *Proc. ICCAS*, 2021, pp. 529–533.